Article
Beitr. Phys. Atmosph., August 1995, p. 233–248
0005-8173/03 0233–16 $ 3.00/0
Vol. 68, No. 3 233

Recent Northern Winter Climate Trends, Ozone Changes and Increased Greenhouse Gas Forcing

by H.-F. GRAF, J. PERLWITZ, I. KIRCHNER, and I. SCHULT

Max-Planck-Institut für Meteorologie, Bundesstr. 55, 20146 Hamburg, Germany

(Manuscript received February 23, 1995; accepted May 26, 1995)

Abstract

Besides the increase in greenhouse gas concentrations and aerosols, considerable trends in ozone concentration were recently shown, with positive values mainly in the upper troposphere, and decreasing concentrations in the lower stratosphere of the Northern Hemisphere middle and high latitudes (WMO, 1992). The data basis consists approximately of 15 to 20 years of observations at various locations. The ozone changes are discussed against the background of observed variations of temperature and circulation during the last decades and are compared with the results of General Circulation Model (GCM) simulations of the effects of the increased greenhouse gas concentration, additional aerosols and the modified ozone profile itself. The observed increased lower stratospheric high latitude westerlies are part of a natural coupled mode of lower stratospheric and tropospheric circulation. This coupled mode has its strongest tropospheric effects over the North Atlantic with increased westerlies, and positive air temperature anomalies over Scandinavia and Siberia. The part of this natural coupled mode which is associated with enhanced polar stratospheric westerlies has increased in intensity during the last decades. A primary contribution to this intensification by the low latitude greenhouse-gas effects is suggested. The observed ozone trends, when integrated into a GCM, do not produce substantial changes in circulation supporting the initial greenhouse gas effects. It is concluded that a comprehensive climate model is needed to study future climate scenarios. This should include atmospheric chemistry in combination with a good representation of the whole stratosphere. It appears most probable that greenhouse-gas effects and ozone concentration are not independent of one another.

Introduction

In this paper we will address the observed changes in stratospheric and tropospheric fields of geopotential and temperature in the light of changes of the concentration and distribution of trace constituents of the atmosphere. In particular, the possible interactions and feedback links between the different changes will be discussed. The results, in part, can be interpreted in terms of coupled modes of the stratospheric and tropospheric circulation.

Using ozone sonde observations at middle and high latitudes of the NorthernHemisphere, considerable trends in ozone concentration were shown, with positive values mainly in the upper troposphere, and decreasing concentrations in the lower stratosphere of the Northern Hemisphere (WMO, 1992). At the same time the additional input of greenhouse gases into the atmosphere continued, possibly also changing the state and behaviour of the atmosphere (e.g. Cubasch et al., 1994b). Calculations of the radiational effects of the changed vertical profiles of the ozone concentration have shown that these are of positive sign and of comparable magnitude to the forcing induced by other prominent greenhouse gases like CO_2, CH_4, CFCs and N_2O during the same time (Wang et al., 1993). First estimates of the possible effect of the increased concentration of tropospheric aerosols forming from SO_2 on the radiative forcing (Kiehl and Briegleb, 1993) and climate (Taylor and Penner, 1994; Roeckner et al., 1995)) became available only recently. These estimates suggest a general reduction of the net greenhouse effect near the earth's surface with strong regional modifications according to the nonhomogeneous distribution of the sulphate aerosols.

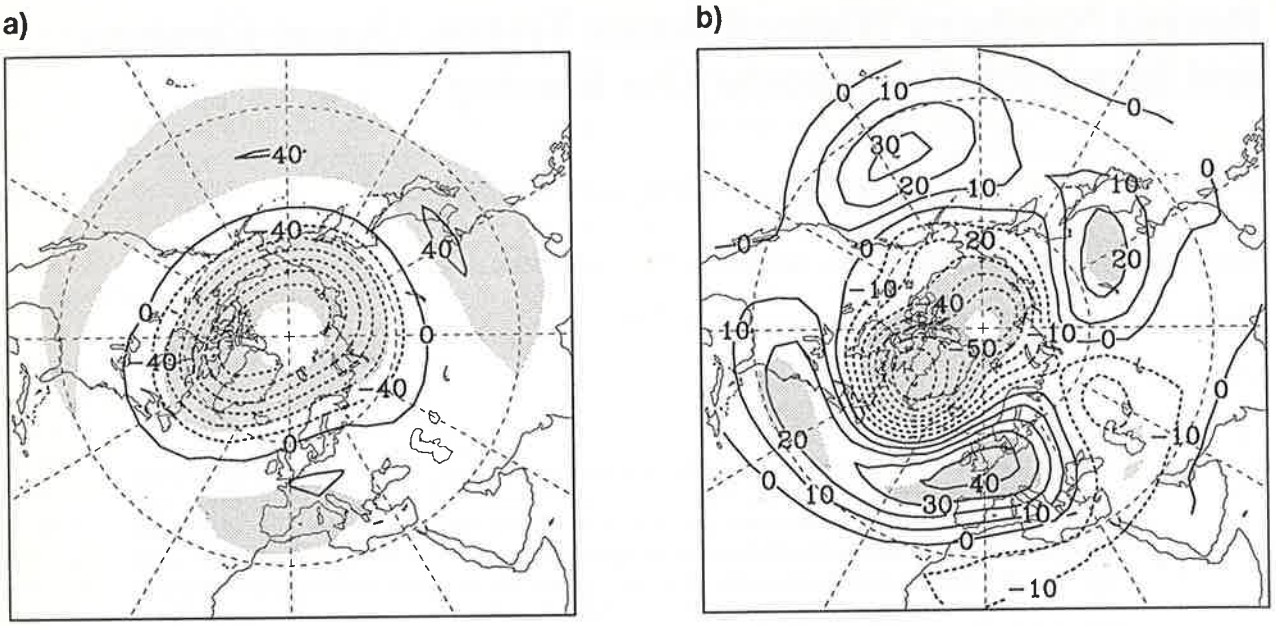

Figure 1 Coupled mode of a) 50 hPa and b) 500 hPa geopotential height anomalies [gpm] of Northern Hemisphere in winter (DJF), determined with the Canonical Correlation Analysis (Perlwitz and Graf, 1994). Regions where the coupled mode explains more than 20 % of local variability are shaded.

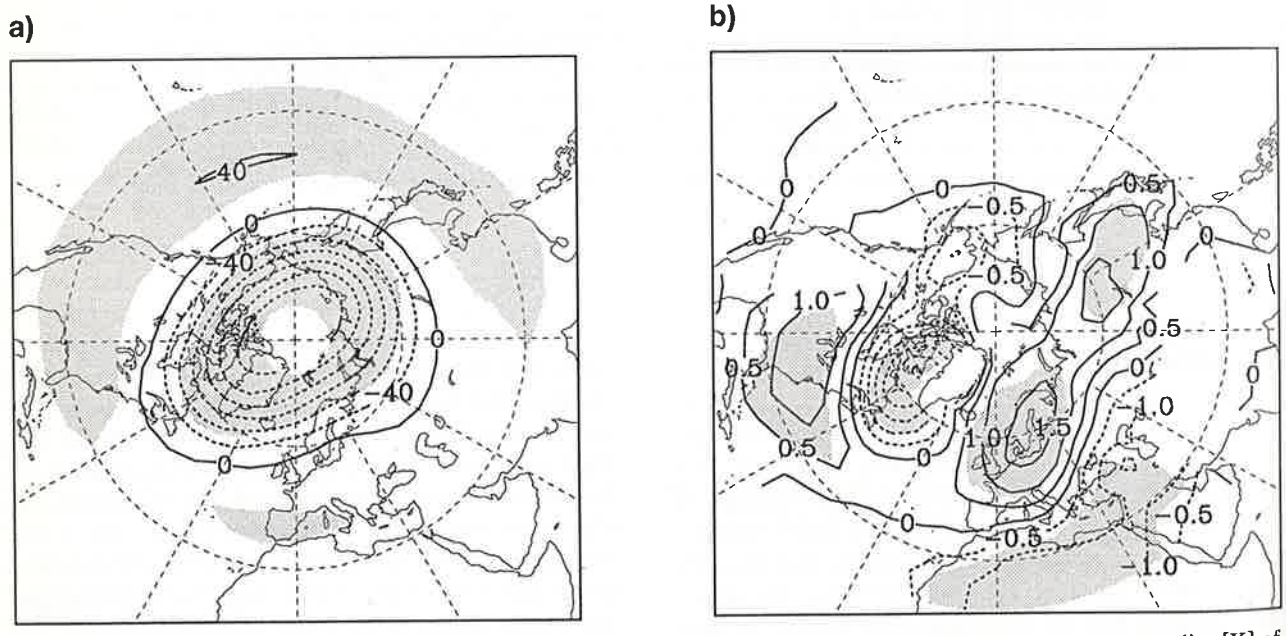

Figure 2 Coupled mode of a) 50 hPa geopotential height anomalies [gpm] and of the b) 850 hPa temperature anomalies [K] of the Northern Hemisphere in winter (DJF), determined with the Canonical Correlation Analysis (Perlwitz and Graf, 1994). Regions where the coupled mode explains more than 20 % of local variability are shaded.

The structure of the paper leads, after a brief discussion of the dynamic coupling of stratospheric and tropospheric winter circulation, to an investigation of the observed recent trends in temperature and geopotential for the stratosphere and troposphere. These trends then are discussed on the basis of experiments with General Circulation Models for changed trace gas concentrations.

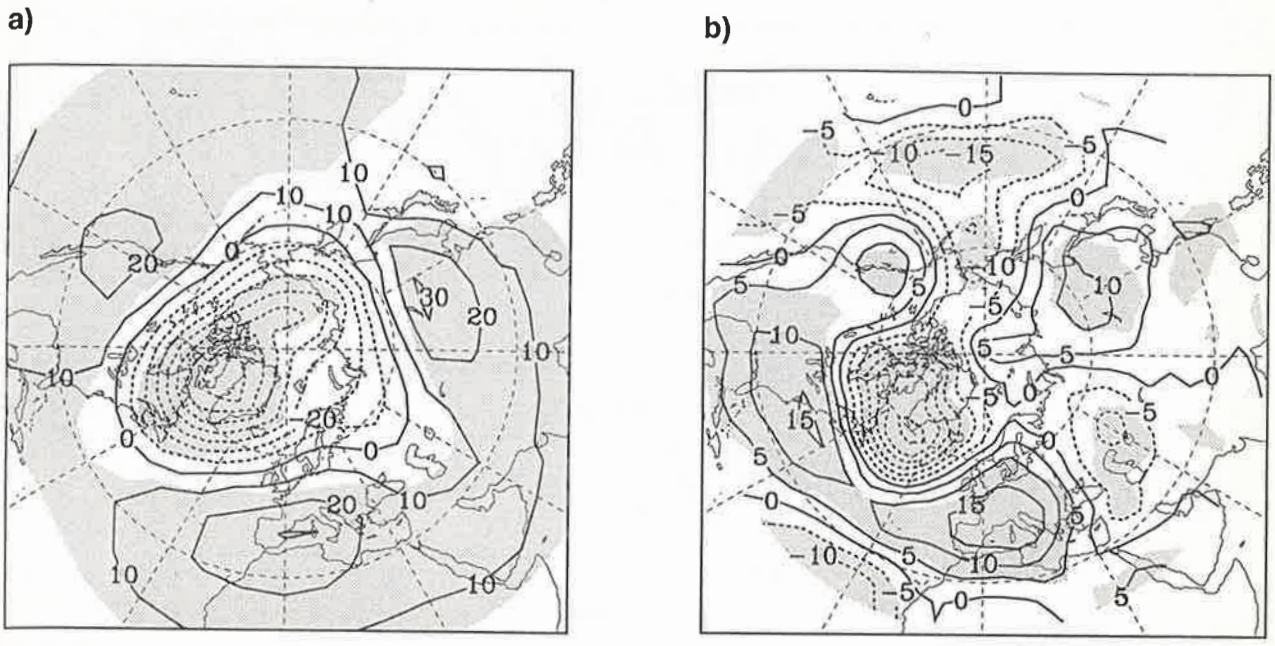

Figure 3

a) Local linear trends of winter mean geopotential heights [gpm/dec] of the 50 hPa level (time period: DJF 1957/58 -1991/92). Regions where the regression coefficient is different from zero at the chance of error of 10% are shaded.

b) Same as in Figure 3a, but for the 500 hPa geopotential height [gpm/dec].

A Coupled Mode of Tropospheric and Stratospheric Circulation

In a recent study Perlwitz and Graf (1994) discussed coupled modes of the lower stratospheric and tropospheric circulation. These modes were estimated by application of the Canonical Correlation Analysis in the phase space of Empirical Orthogonal Functions to observations. The most prominent coupled mode is one they termed "baroclinic mode". It consists of variations in the strength of the lower stratospheric winter vortex that are coupled with anomalies in the tropospheric geopotential fields. These are most pronounced in the North Atlantic area (Figure 1). In the figures those areas are shaded where the coupled mode explains more than 20 % of local variability. The circulation anomalies resulting from the altered geopotential field are then responsible for specific temperature anomalies in middle and high latitudes of the Northern Hemisphere (Figure 2). Since it is a linear coupled mode, the patterns shown in Figures 1 and 2 may be multiplied either with positive or with negative factors corresponding, for instance, to a strong or to a weak vortex. The positive enhancement of this mode was found to be responsible (Graf et al., 1993) for the continental "midlatitude winter warming" (Robock and Mao, 1992) observed after violent tropical volcanic eruptions.

Linear Trend Analysis

In this section we shall briefly discuss the results of an analysis of the linear trends of the geopotential height and temperature of standard pressure levels during the last 35 years. The stratospheric data are obtained from the Stratospheric Research Group of the Meteorological Institute of the Free University of Berlin, the tropospheric data are analyses of the National Meteorological Center (NMC) of the USA, and surface air temperature data were obtained from the Climate Research Unit of the University of East Anglia. The data sets are of different length in time. In order to use the full information we consistently used the complete data sets as shown in the legends of the figures. The stability of the patterns was tested with reduced data sets. The trend analyses were performed in such a way that a linear regression was computed of the observed data (mean of winter, DJF) versus time at every data gridpoint. The regression coefficient is given in unit per decade. It can be statistically tested against the variability of the data during the period of observation by applying a local t-test. Those areas where the regression coefficient is different from zero at a chance of error of 10 % or less are shaded. For the troposphere the individual winters were taken to be independent, while in the stratosphere as a conservative estimate only every

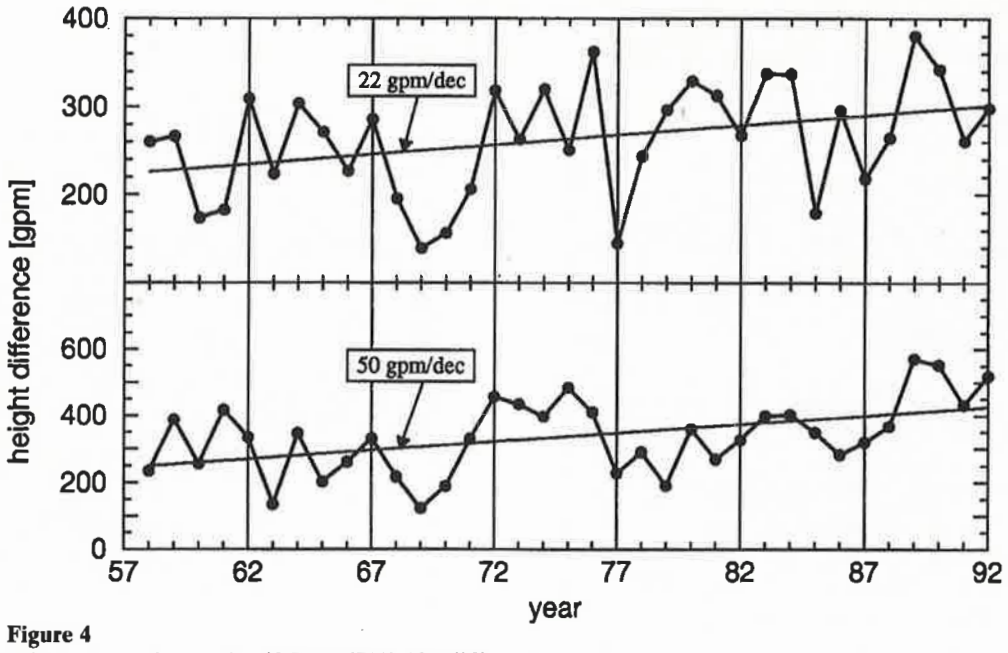

Figure 4
Winter mean time series (DJF 1957/58-1991/92):
Upper panel: Difference of the zonally averaged 50 hPa geopotential height between 50 °N and 60 °N corresponding to the strength of the polar night jet, together with the linear trend function. T-test value for the linear regression coefficient is equal to 2.21.
Lower panel: Difference of the 500 hPa geopotential at two gridpoints ([45 °N 10 °E] minus [60 °N 60 °W]), together with the linear trend function. T-test value for the linear regression coefficient is equal to 3.08.

second winter is independent, i.e. the degree of freedom was reduced by a factor of two for the stratospheric data. This statistical test only means that the parameter considered changed its mean value during the time of observation, it cannot say anything about the significance of the change on the background of general climate variability.

The trends found in the geopotential heights of the 50 hPa level (Figure 3a) are dominated by a strong decrease of the geopotential height in polar latitudes of the Northern Hemisphere. The maximum is reached with minus 80 gpm per decade over the Davis Strait. This means that the "polar funnel" is deepened. In the lower latitudes, on the other hand, a slight increase in the geopotential of the 50 hPa layer is observed. The zonal mean of this pattern indicates an intensified meridional gradient 50 °N minus 60 °N of the geopotential in the lower stratosphere of 22 gpm per decade, Figure 4 (upper panel). This implies a strengthening of the lower stratospheric polar winter vortex (Perlwitz and Graf, 1994).

In the troposphere the strongest geopotential trends are found in midlatitudes and right under the stratospheric low over Greenland and the Davis Strait. The increasing geopotential of the lower and middle troposphere is restricted to North America, the North Atlantic and Europe (Figure 3 b). The pattern suggests stronger westerlies over the Northwest Atlantic and stronger south-westerlies over the Northeast Atlantic. A time series of the geopotential difference between the two points over the North Atlantic area with the maximum anomaly amplitude (but of different sign) is given in Figure 4 (lower panel). The forced regional geopotential gradient might well correspond to a higher frequency and/or strength of cyclones over the North Atlantic with better conditions for the mixing of lower stratospheric and upper tropospheric air. This would then lead to an increase of ozone in the upper troposphere mainly over the North Atlantic and Europe. Around 60 °E in the middle troposphere a trough develops that will be responsible for the advection of arctic dry and cold air into the eastern Mediterranean.

The lower stratospheric temperature is characterized by a general decrease in temperature (Figure 5a) of the order of mostly less than 1 K per decade. The regression coefficients pass the 90 % significance limit only in some areas. At most places the signal to

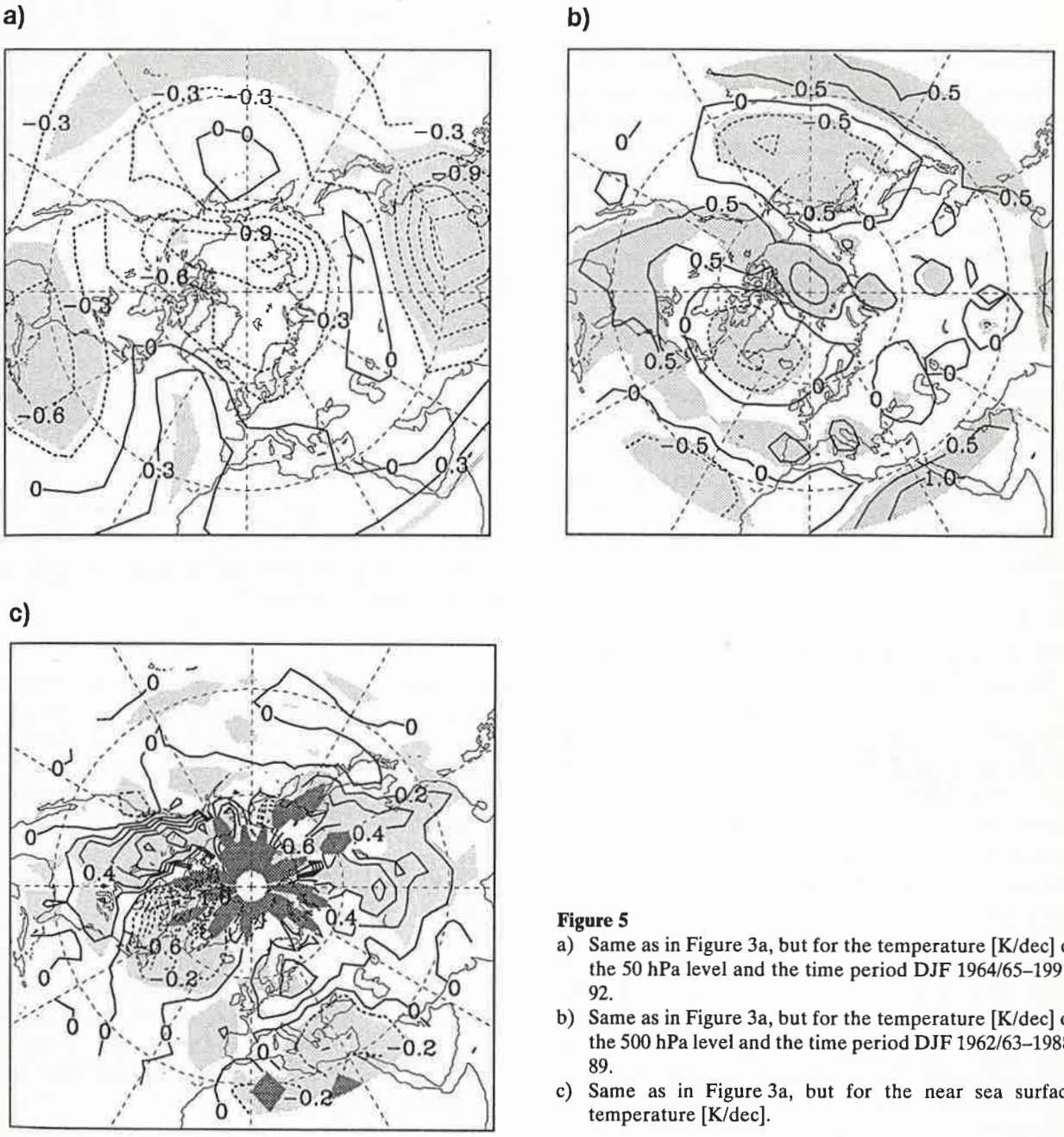

Figure 5

a) Same as in Figure 3a, but for the temperature [K/dec] of the 50 hPa level and the time period DJF 1964/65–1991/92.

b) Same as in Figure 3a, but for the temperature [K/dec] of the 500 hPa level and the time period DJF 1962/63–1988/89.

c) Same as in Figure 3a, but for the near sea surface temperature [K/dec].

noise ratio is too small. Significant negative trends exceeding – 1 K per decade occur near the North Pole and over Southeast Asia. Weaker, but still significant, decrease in stratospheric temperature is observed over the Caribbean and over the subtropical northern Pacific ocean.

Significant positive tropospheric temperature trends in part geographically correspond to the negative trends in the lower stratosphere (Caribbean and southerly North America, near the North Pole, and parts of the subtropical North Pacific). This is in agreement with the troposphere-stratosphere compensational principle, i.e. an increase in tropospheric temperature leads to a higher tropopause and thus to a cooler lower stratosphere. In the middle troposphere trends are quite patchy. Mostly values of the order of 0.5 K per decade are found (Figure 5b). The 850 hPa temperatures (not shown here) suffer from problems due to the mountain influence on the observations. Reliable data are thus only partially available. Here positive trends are well established over Europe and the east of North America of the order of 0.5 K per decade, and cooling is observed over North Africa and over the middle to lower latitudes of the Atlantic and Pacific oceans.

The observed near surface temperature trends shown in Figure 5c have a very interesting structure. While there are large areas of significant warming during the 1957/58 through 1991/92 winters in middle latitudes over the northern continents, significant cooling of the order of – 0.5 K per decade takes place over the Northwest Atlantic, including Labrador and Greenland and, somewhat weaker, also over the eastern Mediterranean and North Africa. In the polar area the data coverage is too incomplete to allow the calculation of trends. The areas with more than 10 years of missing data are shaded dark in the figure. A comparison of the middle tropospheric temperature trends with those near the earth surface shows that the patterns have little in common, except the decreasing temperature near Greenland. The positive temperature trends over the midlatitude continents are a phenomenon, which is most pronounced in the lower troposphere.

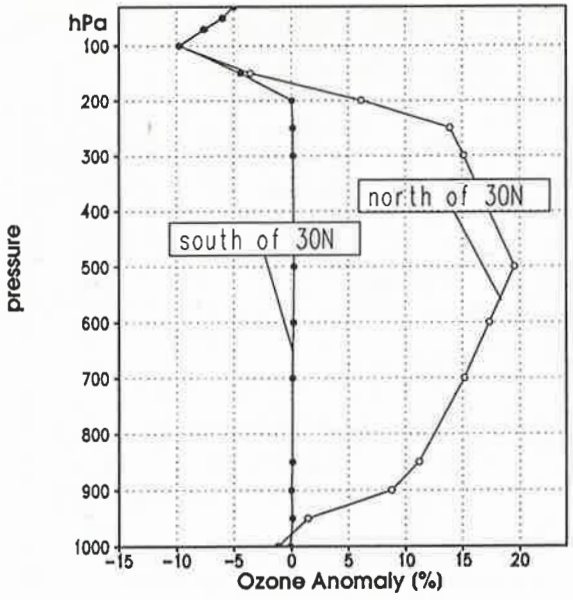

Figure 6 Ozone anomalies [%] used as forcing in the experiment with ECHAM3-T21.

The Modelled Effect of Changed Trace Gas Concentrations

Using the observations alone there is no way to determine what are the reasons for the trends or to prove that they are forced at all. The observed ozone anomalies (WMO, 1992) may have been due mainly to changes in atmospheric circulation (which also can be forced by other trace constituents like the greenhouse gases) or they may have been due primarily to chemical processes leading to ozone changes, producing climate anomalies only secondarily. An appropriate tool to study this problem is the general circulation model (GCM) used at the Max-Planck-Institut in Hamburg. This model has shown its capability to describe climatic anomalies like those resulting from enhanced stratospheric aerosol after violent volcanic eruptions (Graf et al., 1993) and it was used in computing the effect of different greenhouse-gas scenarios (Cubasch et al., 1994a), El Niños (Latif et al., 1993) and also of the burning oil wells during the Gulf War (Bakan et al., 1991). The model, including modern standard physics, is a 19 level T21 spectral model with the top of the atmosphere at 10 hPa and a horizontal resolution of about 5.6 degrees. A detailed description is given in Roeckner et al. (1992) and DKRZ (1992).

We studied the modified model climate in all transient and time slice greenhousegas experiments that have been conducted at MPI in the following ways: with different ocean circulation models coupled to the atmosphere (ECHAM1/T21 and LSG: Cubasch et al., 1992; ECHAM2/T21 and OPYC: Lunkeit 1993); with enhanced resolution (30 year time slice at $2 \times CO_2$ and $3 \times CO_2$, ECHAM3/T42 with SST from ECHAM1/T21: Cubasch et al., 1995); with an earlier start of the integration (1935, ECHAM1/T21 LSG: Cubasch et al., 1994b) in order to overcome the "cold-start" problems (Hasselmann et al., 1992); with sulphate aerosol experiments and with combined experiments (ECHAM 1/T21 with mixing layer ocean: Roeckner et al., 1995) of sulphate aerosol and greenhouse-gas forcing. In addition to these model calculations we performed a new series (ECHAM3/ T21 climate SST) of integrations in which the observed change in ozone distribution over the Northern Hemisphere was assumed to be the forcing factor.

Ozone Forcing

A simplified vertical ozone trend structure was used to force the ECHAM3/T21 version of the Hamburg climate model. The original vertical ozone profile of the model (which is fixed at every gridpoint, there is no transport of ozone) was changed so that the middle and upper tropospheric ozone concentration was enhanced by 15 to 20 % north of 30 °N, and globally the lower stratospheric ozone concentration was reduced by up to 10 % peaking at 100 hPa (Figure 6). This change of the ozone concentration is considered to be representative for the difference

between the 1960's and the 1990's. We used zonal mean forcing functions because insufficient ozone sonde observations (Bojkov et al., 1994) exist to provide us with the necessary vertical profiles for three dimensional trends, and the TOMS data (Stolarski et al., 1992) only give the total column values. It was shown before with the greenhouse-gas experiments and also with forcing by volcanic aerosol (Graf et al., 1993) that globally homogeneous or zonal mean forcing can lead to strong non-homogeneous signals due to changes in the planetary wave pattern.

The first problem to be solved is whether the changes in ozone concentration lead to a forcing strong enough to change the atmospheric circulation considerably. We conducted a total of nine independent 60-day ozone-anomaly integrations, each integration starting with the initial data of another January 1st of a multiyear control integration without any additional forcing. For this experiment the sea surface temperature was prescribed climatologically. Generally, from the thermodynamic point of view, our 60 day forcing time of the individual integrations is not quite long enough to reach an equilibrium effect. The characteristic time of the lower stratosphere to external diabatic forcing is of the order of two to three months. But, if the changes in ozone concentration mainly are due to advection, the autocorrelation function of the lower stratospheric geopotential may serve as an estimate of the characteristic forcing time. This parameter has significant positive values only in the tropics and in very high latitudes north of 70 °N. In the middle and high latitudes of the Northern Hemisphere, however, there is no autocorrelation left after about two weeks. This means that changes of the large scale circulation dominate the temporal course of temperature. Since ozone is also subject to advection, the forcing time is much smaller than the diabatic response time of the lower stratosphere, except inside strong and stable vortexes which, if not geographically fixed (due for example to orographic forcing) will also move with the mean flow. A GCM more appropriate to the problem would require also transport (and chemistry) of ozone in the lower stratosphere and upper troposphere. Such models are currently being developed, but are not yet available.

We had to use January 1st initial data since in the computing centre library so far the initial data of every sixth month are stored. Although we would have liked to start, say in October or November, we chose January as a compromise between the economic use of computer time and the need to achieve a representative result. It may be speculated that stratospheric ozone depletion is a primary reason for the polar cooling in northern early winter as identified by Labitzke and van Loon (1994). Kodera and Yamazaki (1994) showed that a strong Polar Night Jet (PNJ) in early winter in the middle stratosphere tends to move downward in the course of the season. Thus, an initial cooling might be the seed for a strong PNJ later on in lower stratospheric altitudes and for changes in the planetary wave patterns of the troposphere. This investigation was carried out with limited data, based mainly on composites. Our own investigations of the stability of the observed high latitude temperature anomalies at an isentropic surface, however, have shown that there is no autocorrelation left after a few weeks (not shown here). This means that even though the reduced ozone may lead to initial cooling in high latitudes in the middle stratosphere at the beginning of winter, this effect will not have any significant impact on the stratosphere during the polar night. In addition, Randel and Cobb (1994) showed the zonal mean ozone and temperature trend to be strongest at midlatitudes during January and February. Thus, our GCM results are aimed as a check for the general efficiency of the observed ozone changes as a climate forcing element. If the strongest observed changes of the ozone concentration cannot produce a significant climate signal, then, probably, nor will the smaller variations during the other seasons.

The instantaneous forcing from our change in ozone concentration (Figure 6) is shown in Figure 7. Here the flux anomalies in longwave thermal and shortwave solar radiation are shown for the 140 hPa layer of the Climate Model in January. This model layer roughly represents the layer separating the stratospheric part with ozone decrease from the troposphere with increasing ozone concentration. The mean effects from clouds etc. are included in the computations. Due to less solar absorption in the reduced stratospheric ozone the troposphere receives more shortwave radiation outside the polar night region. This leads to slightly enhanced heating rates in the troposphere where the absorption of shortwave radiation is increased (not shown here). The ozone mixing ratio is smallest in the tropics with increasing values towards the poles, and the solar intensity is highest in low latitudes. Due to this combination of the underlying ozone climatology and the solar radiation intensity, the maximum radiative effect is in midlatitudes. Because of the tropospheric heating and expansion in addition to the reduced absorption of solar radiation in the

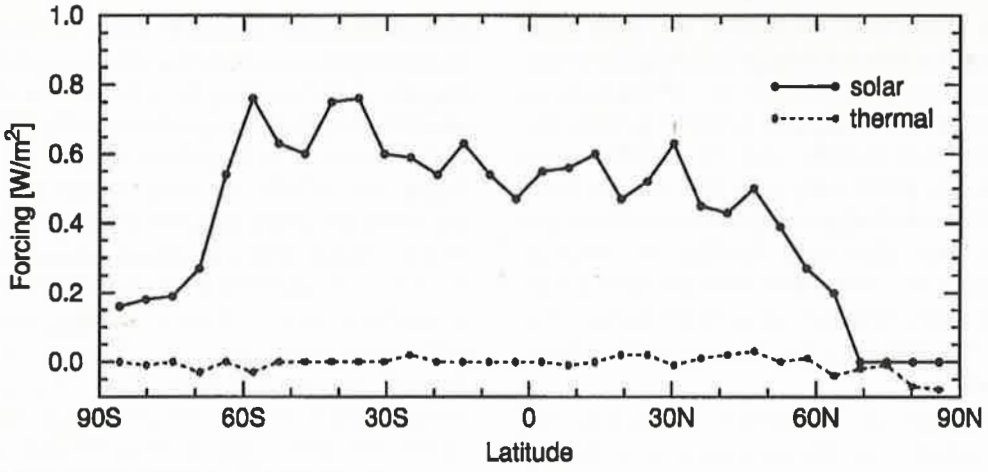

Figure 7 Instantaneous radiative forcing in the 140 hPa layer due to ozone change from Figure 6.

stratosphere, the lower stratosphere initially cools down at rates of 0.05 K per day in places where sunlight is present. In the polar area very weak warming occurs possibly due to sinking motion following small additional cooling because of decreased absorption of longwave radiation in the troposphere.

We studied the model's effects on the vertical ozone profile changes for the days 10 to 30 (i.e. late January) and days 40 to 60 (i.e. late February) of our nine independent 60-day integrations. For the shorter forcing time the analyzed mean anomalies are far from being significant. In the single experiments relatively strong anomalies occur from the mean of all 30 control periods (i.e. the mean of all late January periods of the 30 year control integration, which represent the "model climate"). Anomalies on a similar scale also occur in the individual experiment minus control periods, which represent the "weather disturbance", possibly influenced by the initial conditions. This means that the atmosphere behaves in a rather chaotic manner with very small anomalies in the forcing, resulting in strong, but unforeseeable and non-systematic changes in circulation and temperatures.

The results now discussed are anomalies of the mean model results for the days 40 to 60 from the respective nine control runs without any changes to the ozone profiles. Again, the response is rather weak and only of marginal, if any, statistical significance. In general the atmosphere shows a wave number one response to the zonal symmetrical forcing of the changed vertical ozone profile in the stratosphere (Figure 8). Figure 9a shows the results of a harmonic analysis for zonal wave number one amplitudes of the 70 hPa geopotential in the control runs (broken lines, one standard deviation shaded) and in the experiment (solid lines, error bars indicating one standard deviation). The same analysis for the temperature of the same pressure level is shown in Figure 9b. The maximum differences between control and ozone experiment occur near the polar circle of the Northern Hemisphere, where the temperature amplitude reaches 8 K and the geopotential wave number one has a mean amplitude of about 90 gpm. But at the same latitude the variability of the amplitudes is highest, and thus the differences found are not statistically significant. In Figure 10 the results of the harmonic analysis are shown for the single realizations at a latitude of 58 °N. Here the strong variability becomes clear again for the amplitudes. The phases of the zonal wave one (defined as the longitude of the first maximum counted from the Greenwich meridian eastwards) show on the other hand only slight and non-systematic changes.

In six out of the nine cases the phase of the wave is nearly the same while the amplitude varies. In one case there is no obvious structure, and in two cases the wave is out of phase with the other cases. Therefore, the zonal and temporal mean of the anomalies in a meridional vertical projection (not shown here) do not show any significant structure. Although the absolute anomalies of a longitude/latitude projection (for example, of the geopotential in the lower stratosphere) are quite large (Figure 8a), showing a clear zonal wave number one structure with a minimum over the North Atlantic and a maximum over Alaska, the statistical evidence remains mediocre, since the one standard deviation value is not exceeded except at a few points. In the middle and high latitudes of the Northern Hemi-

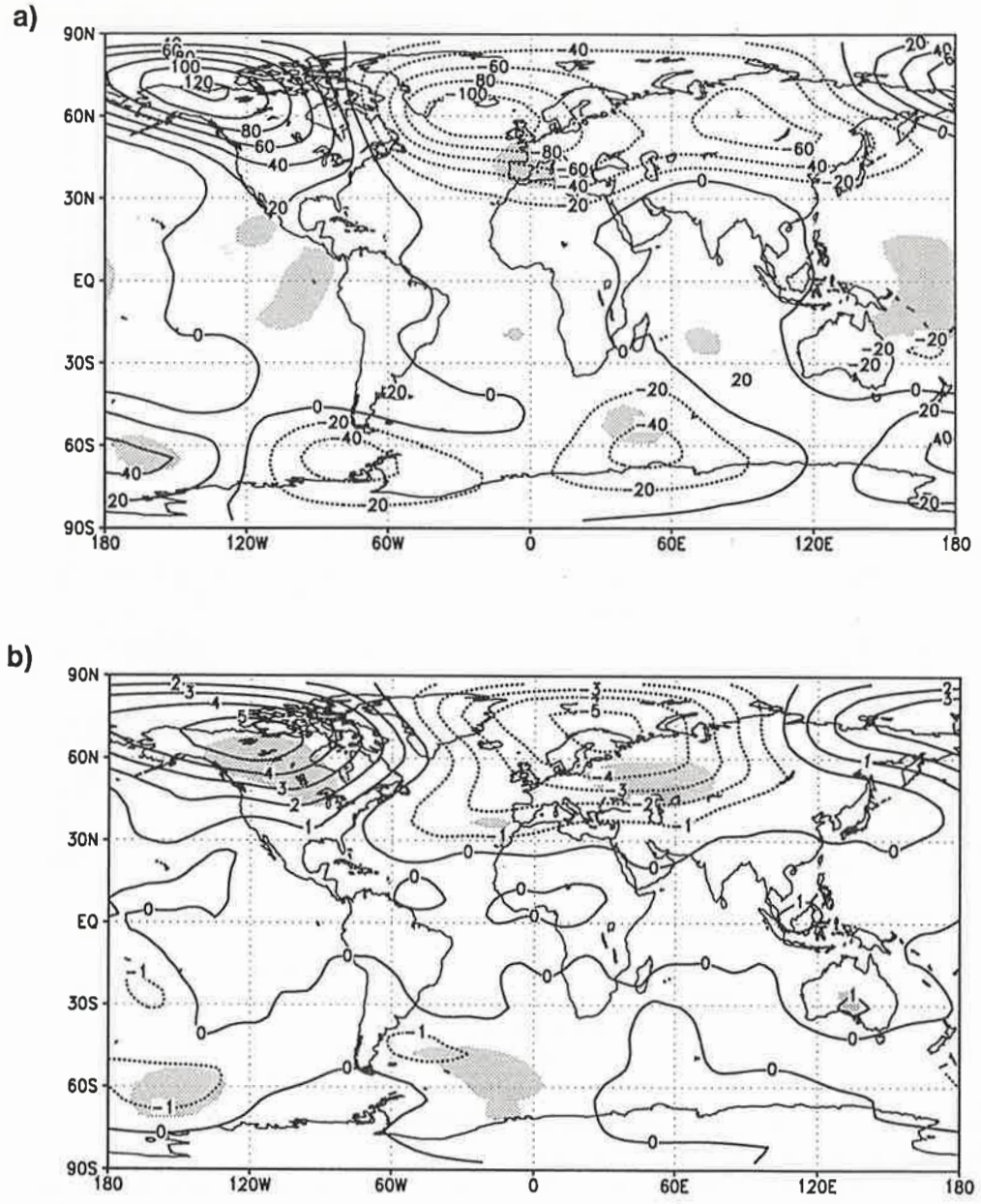

Figure 8

a) Mean geopotential height anomalies [gpm] of the 70 hPa layer (days 40 to 60) of nine experiments with ozone forcing starting at 1st of January. In shaded areas the mean amplitude exceeds one standard deviation of the control run value.

b) Same as in Figure 8a, but for temperature anomalies [K].

sphere, where the largest amplitudes are found, the natural variability is too strong to be exceeded even by values of the order of 100 gpm. On the other hand, in the tropics, where the model variability is very small, the anomaly amplitudes are too small to be physically meaningful although they have higher statistical significance. The anomalies of the lower stratospheric temperature as seen in Figure 8b provide evidence for a clear barotropic response of the atmosphere over North America. In middle and high latitudes the anomaly fields of geopotential and temperature are largely congruent. Over the North Atlantic and Europe, however, clearly baroclinic effects dominate as can be seen from the shift of the anomaly patterns for geopotential versus temperature.

The surface air temperature is another important parameter of climate. This parameter is restricted to

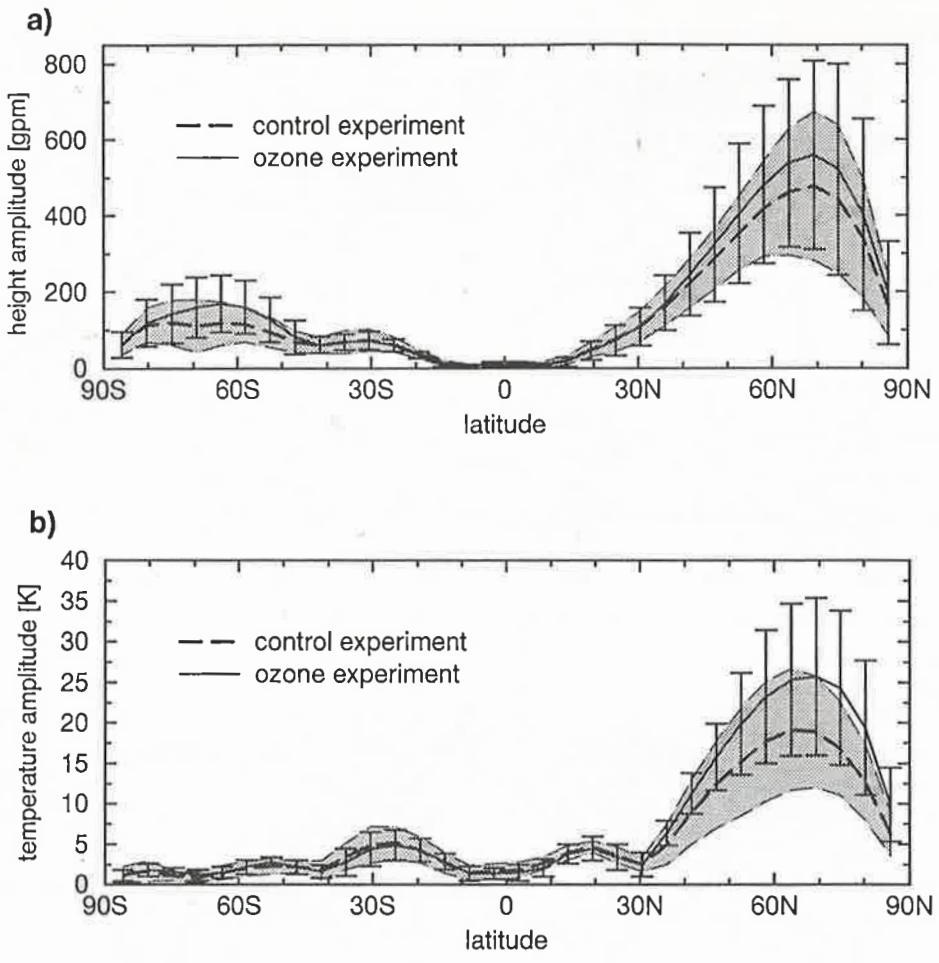

Figure 9

a) Mean zonal wave number one amplitudes of the 70 hPa geopotential height of the control runs (broken line, one standard deviation shaded) and of the experiments (solid line, error bars indicating one standard deviation).

b) Same as in Figure 9a, but for the temperature of 70 hPa layer.

small amplitudes close to the ocean surface due to the prescribed sea surface temperature. Over land and ice, however, the temperature follows the energy budget. Figure 11 shows quite substantial temperature anomalies in middle and high latitudes, but the statistical significance is low due to the bad signal to noise ratio. The north polar warming in the lower troposphere is mainly due to an increase in cloud cover in the lower troposphere (not shown here). Therefore above the boundary layer no temperature signal is seen.

The circulation in the lower stratosphere, which would be of major interest if there were feedback between ozone concentration changes and wind regimes, also does not show any response of statistical significance. The simulated anomaly fields are physically consistent, but obviously the power of the forcing is not strong enough to overcome the chaotic nature of atmospheric circulation.

Forcings other than Ozone

Since all observations include effects from greenhouse gas, tropospheric aerosol and ozone forcing, it remains unclear which of these effects, if any, is responsible for the observed features. We therefore also studied the trends being produced solely by greenhouse gas forcing. These experiments include, among others (see above), the IPCC scenario A integrations with the Hamburg Large-Scale Geostrophic (LSG) ocean coupled to the T21 ECHAM1 atmospheric circulation model (Cubasch et al., 1994a). The analysis of all simulations led to comparable results. Here we prefer to present the "Scenario A" results only since this is still the standard experiment at MPIM. The model was initiated with the 1985 CO_2 concentrations. Starting from an earlier time of industrialization (Cubasch et al., 1994b) gives similar results one decade earlier.

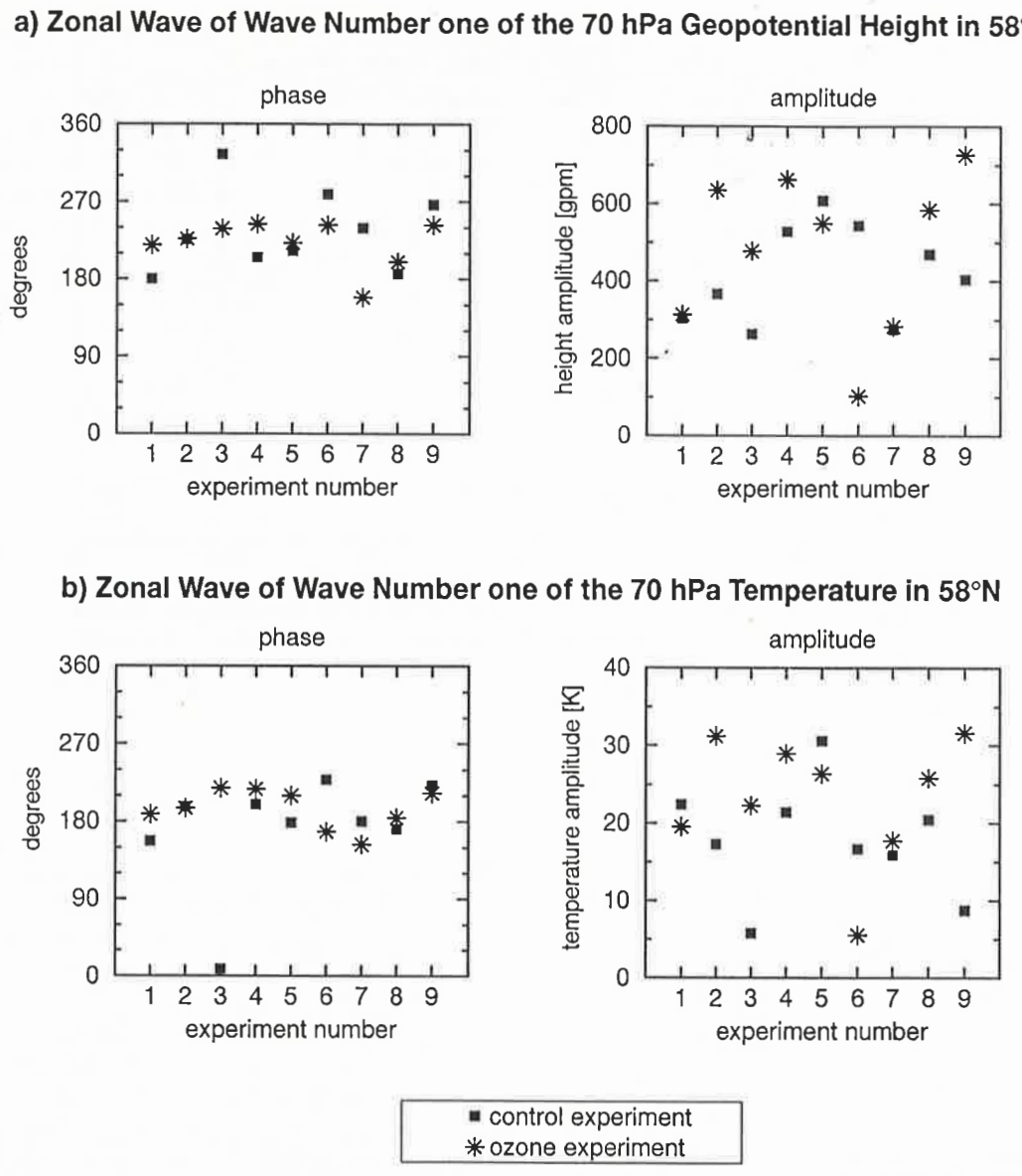

Figure 10

a) Phases (left panel) and amplitudes (right panel) of zonal wave number one in 58 °N of the geopotential height of the 70 hPa layer for the nine single control runs (filled squares) and nine single experiments (stars).

b) Same as in Figure 10a, but for the temperature of the 70 hPa layer.

At the beginning of the integration the atmospheric changes are only weak and mostly insignificant. Therefore in Figure 12 the simulated trends for the model winter means (DJF) for the integration years 29 to 59 are shown, corresponding to IPCC Scenario A CO_2 concentrations for the years 2014 to 2044. The 30-year trends for earlier model periods vary from period to period. The main stable features found from the beginning of all integrations, however, are an increase of the geopotential height in lower latitudes and a slight decrease near the North Pole in the lower stratosphere. These basic structures of the simulated trends were found in all transient greenhouse gas experiments (see above) with small differences in amplitude and timing and they agree fairly well with the observations from Figure 3 (note the changed isoline distance between Figures 3 and 12 in the stratosphere) for the North Atlantic area.

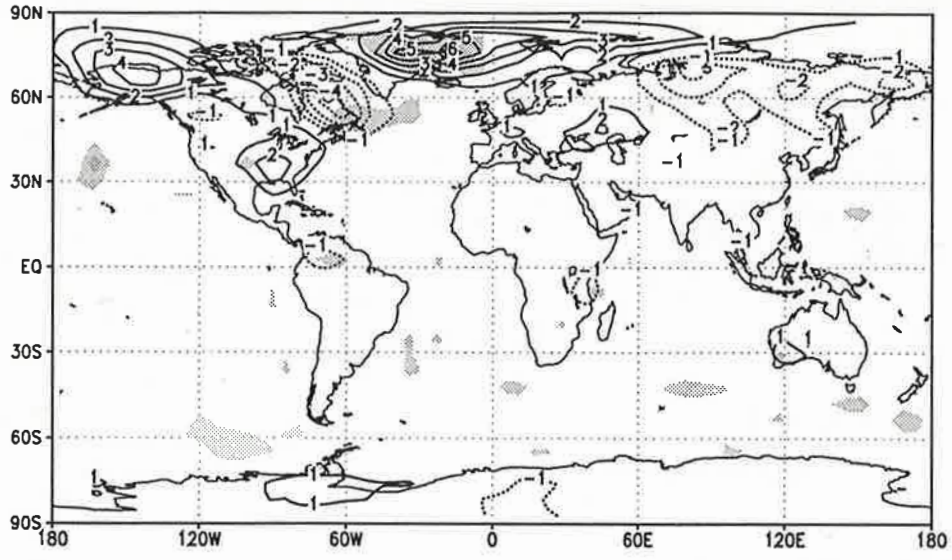

Figure 11 Mean near surface temperature anomalies [K] (days 40 to 60) of nine experiments with ozone forcing starting at 1st of January. In shaded areas the mean amplitude exceeds one standard deviation of the control run value.

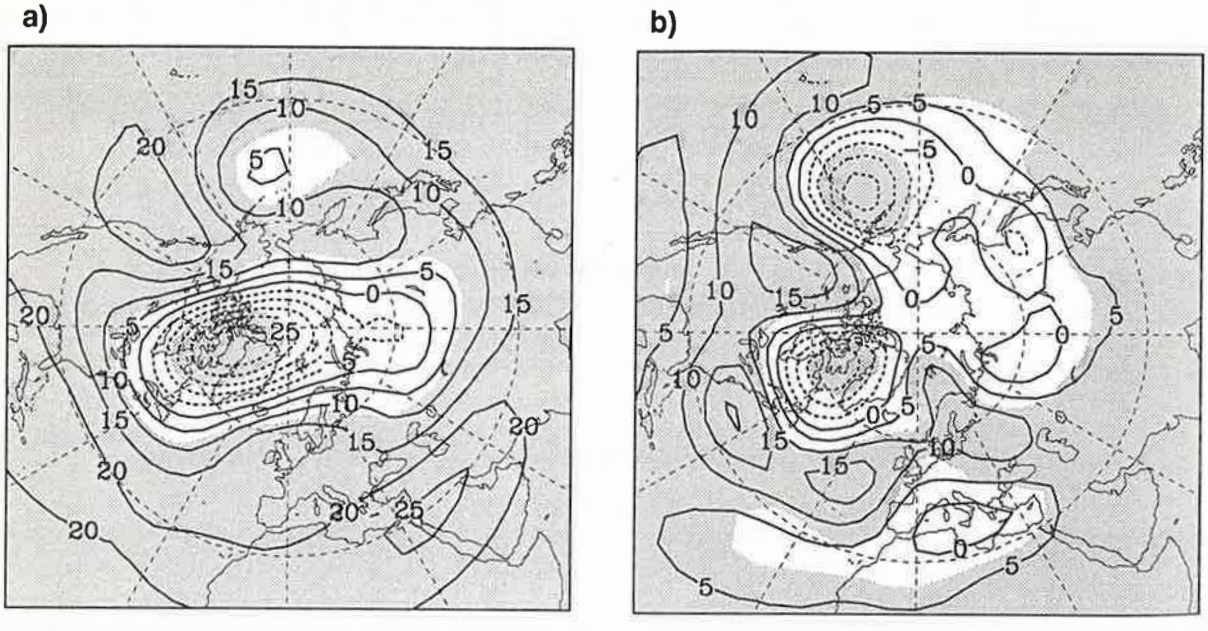

Figure 12

a) Local linear trends of winter mean 50 hPa geopotential heights [gpm/dec] of the IPCC Scenario A CO_2 integrations with the LSG/ECHAM1 T21 model (DJF 29/30–58/59). Regions where the regression coefficient is different from zero at the chance of error of 10 % are shaded.

b) Same as in Figure 12a, but for the 500 hPa geopotential height [gpm/dec].

In all experiments, shortly before reaching CO_2 concentrations double that for 1985 the response structure changes dramatically, then giving the strongest warming over the North Pole. This means that, at least in the model integrations, the trajectory of climate is highly non-linear. The features modelled for a $2 \times CO_2$ scenario do not develop in a linear manner from the undisturbed patterns.

In the middle troposphere, the geopotential trend associated with the baroclinic mode of troposphere-stratosphere circulation coupling is also enhanced. The main features are found in observations as well as in the model results: negative trends of geopotential height over Greenland and the Davis Strait (which are stronger in the observations) and over the North Pacific (which are stronger in the model) and positive trends over the east coast of North America. The positive trend observed over western Europe, however, is shifted westward to the Atlantic in the model compared to observations. The latter is probably due to problems with the ocean circulation in the Mediterranean.

Although the mean structure of observed and simulated trends from Figures 3 and 12 have some similarity, there exist also great differences. The negative geopotential trend in the lower stratosphere, now well established with its maximum over the Davis Strait as in the observations (Figure 3), is smaller than in the observations by a factor of three. Also, it is observed some decades earlier (i.e. at a lower CO_2 concentration) than simulated. Possibly the greenhouse gas forcing from CO_2 equivalents alone is not able to explain the climatic changes in higher latitudes. Other greenhouse gases have to be treated in a more specific way in order to study their individual contribution to the total greenhouse effect. The changes in ozone associated with the changes in circulation due to the observed and simulated trends, which have been neglected so far in such model simulations, acquire importance in this respect only to the extend that non-linear feedbacks between lower stratospheric circulation, increased greenhouse gas concentration and ozone profile changes are of essential significance. For this purpose ozone has to be treated as a prognostic variable in the model, including chemical reactions and transport. A simple superposition (which neglects all possible feedbacks) of the results of the ozone experiment described above and the results of the greenhouse gas simulations does not lead to a better agreement between model and observation because of the weakness of the single signals.

Neither the ozone nor the greenhouse gas forcing alone is able to reproduce the changes of circulation in high latitudes. However, there may be other factors which have not yet been observed in the experiments (such as the state of the ocean circulation) which are responsible for the differences between observation and simulation. This idea was tested by Cubasch et al. (1994a) who started IPCC Scenario A experiments with different initial conditions of a coupled Ocean-Atmosphere-GCM control run in order to estimate the impact of the initial conditions of the coupled system ocean-atmosphere on the result of greenhouse gas forcing. The main result was shifts in the detection time of a signal, the patterns remain unchanged. Some indication of the possibility of non-linear effects in case of multiple forcing can be found in the model results of an experiment dedicated to the study of combined greenhouse gas and sulphate aerosol effects on climate (Roeckner et al., 1995). The stratospheric data from this experiment were kindly provided by the authors. The results are computed from the last 20 years of 45 year integrations of the ECHAM1/T21 GCM coupled to a mixed layer ocean for a combination of the modern anthropogenic sulphate aerosol with 1.4 times the preindustrial CO_2 concentration (this is about the current value of CO_2 concentration). Figure 13 shows the geopotential height anomalies for the experiment. Where CO_2 is doubled, a very strong large scale lift of the 50 hPa layer takes place, strongest in low latitudes and weakest over the Davis Strait; where a minor increase of CO_2 combined with anthropogenic sulphate aerosol is assumed, the geopotential increase of the lower stratosphere is much smaller (but still significant), and in very high northern latitudes the geopotential decreases. This latter feature is extensive agreement both with recent observations (e.g. Figure 3) and with the transient model results (e.g. Figure 12). Hence it seems clear that we need more complex forcings than simply CO_2 increase to reproduce the change in climate during the recent past.

Concluding Suggestions

Here we want to summarize our suggestions for a possible feedback-loop between the increasing greenhouse effect in the troposphere, the changes of stratospheric and tropospheric circulation and possible links with the ozone trends both in the stratosphere and in the upper troposphere.

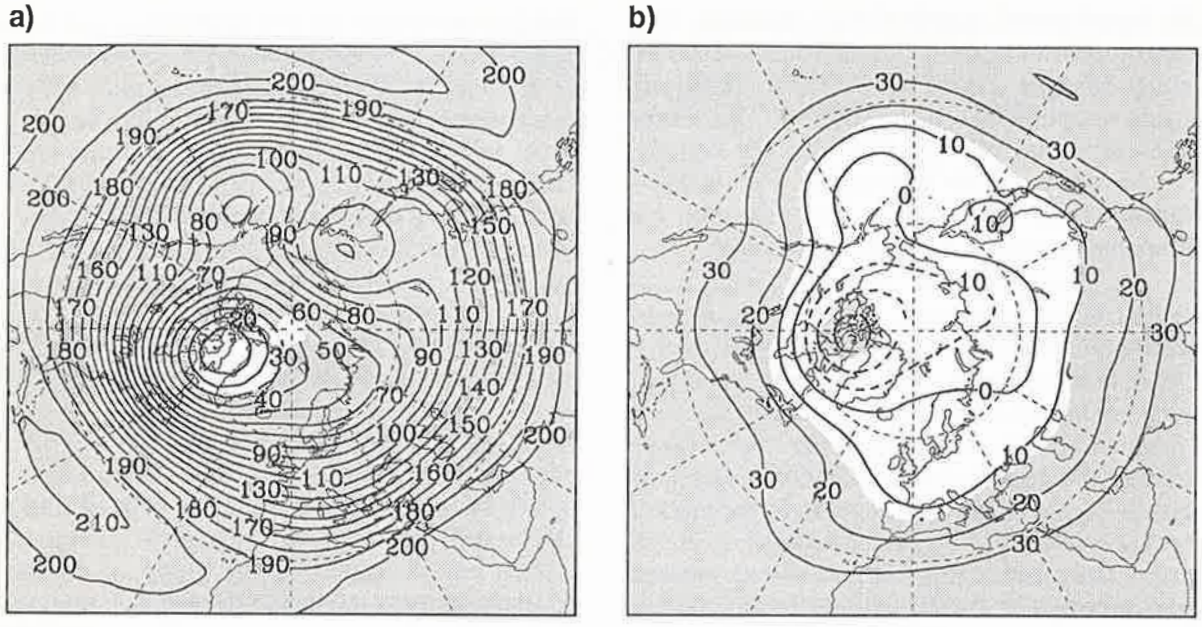

Figure 13

a) Difference between the $2 \times CO_2$ experiment and the control experiment of the winter mean (DJF) geopotential of the 50 hPa layer. The regions where the difference is significant at the 90 % level are shaded.

b) Same as in 13a, but for the difference between the $1.4 \times CO_2 + SO_4$ experiment and the control experiment.

The patterns of the geopotential trends in the lower stratosphere and in the troposphere as well as of the temperature trends in the troposphere observed over the last decades are quite similar to those of a natural coupled mode of tropospheric and stratospheric circulation. This mode is characterized by enforced westerlies in the lower stratosphere in polar latitudes due to amplified geopotential differences between low and polar latitudes in the lower stratosphere. It was recently studied in more detail in Perlwitz and Graf (1994). The tropospheric geopotential anomaly pattern of this mode is determined by a deep trough over Greenland and positive anomalies over the East Atlantic and Western Europe as well as over parts of North America. This leads to stronger westerlies over the Northwest Atlantic and to stronger southwesterlies over the Northeast Atlantic. In connection with these circulation anomalies, temperature anomalies develop with lower than normal temperatures over the northeastern part of North America and the adjacent Northwest Atlantic. Northern Eurasia then becomes warmer than normal. It is suggested that the increased geopotential differences over the North Atlantic may also enhance the power of convection in North Atlantic storm systems, and therefore increase the possibility of mixing of ozone-rich stratospheric air to the upper troposphere. Such a process was successfully modelled recently by Ellis et al. (1994).

Under the influence of the effect of the combined greenhouse gases it is expected that the tropospheric temperature increases and, as an expression of the tropospheric-stratospheric compensational principle, the stratosphere cools down. This stratospheric cooling is really observed for the last 30 winters (DJF). In contrast to the temperature trends, in the lower stratosphere the geopotential trends are of different sign. While here in the low- and midlatitudes of the Northern Hemisphere an increase of the geopotential height is observed, over the North Pole the geopotential decreases drastically. This evolution, leading to an enhanced polar vortex in winter, was shown before in Perlwitz and Graf (1994) using the zonal mean difference of geopotential between 50 °N and 60 °N. According to the results of their Canonical Correlation Analysis, the lower tropospheric trends resemble the basic structure of the baroclinic mode of coupled stratosphere-troposphere circulation over the Atlantic and Eurasia, for the geopotential as well as for the air temperature.

Greenhouse gas simulations with general circulation models show the increase in lower stratospheric geopotential in lower latitudes as observed. In middle and high latitudes, however, their amplitudes do not agree with recent observations. This may be due to the neglect of other simultaneously occurring changes in radiatively effective trace

constituents of the atmosphere, like ozone or aerosols or even other mechanisms, such as, for example, the North Atlantic deep water formation. The simulation of the effects of changed vertical ozone profiles in an otherwise unmodified model world did not show conclusive changes in climate. This simple simulation, however, does not include possible feedback effects nor does it include the ozone chemistry and transport. A model simulation is therefore needed that combines both greenhouse gas and ozone effects, possibly supplemented by aerosols. So far, greenhouse gas simulations show trends in the lower stratosphere circulation that may explain at least part of the observed ozone trends. For example the formation of a trough over the Northwest Atlantic leads to more advection of air with low ozone concentration from low to high latitudes over Eurasia. There is also a need to study the circulation change due to the combination of changes of different greenhouse gases, ozone and aerosols in other simulations of the same kind, but with different models, in order to test the accuracy of the results discussed here.

We suggest that the trends observed during the last three decades in geopotential and temperature, both in the stratosphere and in the troposphere are determined by the preferred occurrence of the natural baroclinic mode of coupled stratosphere-troposphere circulation as defined by Perlwitz and Graf (1994). The initial enhancement of the mode may be due to the rise of geopotential in the troposphere as a result of greenhouse gas warming and increased evaporation. This phenomenon, mainly in lower latitudes, also raises the geopotential of the pressure surfaces in the lower stratosphere, while the stratospheric temperature, following the height of the tropopause, falls. The ongoing ozone depletion in the stratosphere may enhance the cooling there in a positive feedback loop (which could not be studied with the climate model currently available) once the polar vortex is strengthened and ozone is increasingly destroyed via heterogeneous chemistry in polar stratospheric clouds. In this respect also the 14 micron ozone absorption band will be important. This is not included in most of the current GCMs. The trough developing over the North Atlantic leads to ozone reduction outside the vortex since air with low ozone concentration is transported northward from lower latitudes. The increased baroclinicity along the edge of the polar vortex may further facilitate the mixing of stratospheric air with high ozone concentration down into the upper troposphere, leading there to additional radiative heating. This again strengthens the meridional geopotential gradient responsible for the enhanced vortex. Finally, together with the higher intensity of the high latitude stratospheric westerlies, the vertical propagation properties of tropospheric planetary wave energy are changed. The result of this intensification of the PNJ is a changed planetary wave pattern in the troposphere as observed in accordance with the baroclinic coupled mode.

Acknowledgements

We are grateful for the kind supply of data sets to Drs. Barbara Naujokat, John Janowiak and Phil Jones and for the aerosol and CO_2 model experiment data to Dr. Erich Roeckner. This study was sponsored by the Bundesministerium für Forschung und Technologie, contract No. 07-KFT-86/2.

References

Bakan, S., A. Clond, U. Cubasch, J. Feichter, H.-F. Graf, H. Grassl, K. Hasselmann, I. Kirchner, M. Latif, E. Roeckner, R. Sausen, U. Schlese, D. Schriever, I. Schult, U. Schumann, F. Sielmann, and *W. Welke,* 1991: Climate response to smoke from the burning oil wells in Kuwait. Nature **351**, 367–371.

Bojkov, R., V. Fidetov, and *A. Shalamjansky,* 1994: Total ozone changes over Eurasia since 1973 based on re-evaluated filter ozonometer data. J. Geophys. Res. **99**, 22985.

Kiehl, J. T. and *B. P. Briegleb,* 1993: The relative role of sulphate aerosols and green-house gases in climate forcing. Science **260**, 311–314.

Cubasch U., B. D. Santer, A. Hellbach, G. Hegerl, H. Höck, E. Maier-Reimer, U. Mikolajewicz, A. Stössel, and *R. Voss,* 1994a: Monte Carlo climate change forecasts with a global coupled ocean-atmosphere model. Climate Dynamics **10**, 1–19.

Cubasch, U., G. Hegerl, A. Hellbach, H. Höck, U. Mikolajewicz, B. D. Santer, and *R. Voss,* 1994b: A climate change simulation starting at an early time of industrialization. MPI-Report No. 124, Max-Planck-Institut für Meteorologie, FRG, 33 pp. (A climate change simulation starting 1935, Climate Dynamics, in press 1995.)

DKRZ, 1992: The ECHAM3 atmospheric general circulation model. Technical Report No. 6., DKRZ Hamburg, FRG, 184 pp.

Ellis, Jr. W., G. Stenchikov, R. Dickerson, S. Kondragunta, A. Thompson, K. Pickering, J. Scala, and *W.-K. Tao,* 1994: Convective enhancement of ozone production based on emissions from the year 2050. AGU Spring Meeting, EOS Supplement, p. 87.

Graf, H.-F, I. Kirchner, A. Robock, and *I. Schult,* 1993: Pinatubo eruption winter climate effects: Model versus observations. Climate Dynamics **9**, 81–93.

Graf, H.-F., J. Perlwitz, and I. Kirchner, 1994: Northern Hemisphere tropospheric midlatitude circulation after violent volcanic eruptions, Contr. Atmos. Phys. **67**, 3–13.

Labitzke, K. and *H. van Loon,* 1994: A note on trends in the stratosphere: 1958–1992. COSPAR Colloquium Series **5**, 537–546.

Latif, M., T. Stockdale, J.-O. Wolff, G. Burgers, E. Maier-Reimer, M. M. Junge, K. Arpe, and *L. Bengtsson,* 1993: Climatology and variability in the ECHO coupled GCM. Tellus **49A**, 351–366.

Lunkeit, F., 1993: Simulation der interanuellen Variabilität mit einem globalen gekoppelten Atmosphäre-Ozean-Modell. Berichte aus dem Zentrum f. Meereskunde (ZMK), No. 8, Reihe A: Meteorologie, 142 pp.

Kodera, K. and *K. Yamazaki,* 1994: A possible influence of polar stratospheric coolings on the troposphere in the Northern Hemisphere winter. Geophys. Res. Lett. **21**, 809–812.

Perlwitz, J. and *H.-F. Graf,* 1994: On the statistical connection between tropospheric and stratospheric circulation of the Northern Hemisphere in winter. MPI-Report No. 134, Max-Planck-Institut für Meteorologie, FRG, 33 pp (J. Climate in press 1995).

Randel, R. J. and *J. B. Cobb,* 1994: Coherent variations of monthly mean total ozone and lower stratospheric temperature. J. Geophys. Res. **99**, 5433–5447.

Robock, A. and *J. Mao,* 1992: Winter warming from large volcanic eruptions. Geophys. Res. Lett. **12**, 2405–2408.

Roeckner, E., K. Arpe, L. Bengtsson, S. Brinkop, L. Dümenil, M. Esch, E. Kirk, F. Lunkeit, M. Ponater, B. Rockel, R. Sausen, U. Schlese, S. Schubert, and *M. Windelband,* 1992: Simulation of the present-day climate with the ECHAM model: Impact of model physics and resolution. MPI-Report No. 93, Max-Planck-Institut für Meteorologie, FRG, 172 pp.

Roeckner, E., T. Siebert, and *J. Feichter,* 1995: Climate response to anthropogenic sulphate forcing simulated with a general circulation model. In: Charlson, R., Heintzenberg, J. (eds.). Aerosol Forcing of Climate. John Wiley and Sons, 349–362.

Stolarski, R. S., R. Bojkov, L. Bishop, C. Zerefos, J. Stahelin, and *J. Zawodny,* 1992: Measured trends in stratospheric ozone. Science **256**, 342–349.

Taylor, K. E. and *J. E. Penner,* 1994: Response of the climate system to atmospheric aerosols and greenhouse gases. Nature **369**, 734–737.

Wang, W.-C., Y.-C. Zhuang, and *R. D. Bojkov,* 1993: Climate implications of observed changes in ozone vertical distributions at middle and high latitudes of the Northern Hemisphere. Geo. Res. Lett. **20**, 1567–1570.

WMO, 1992: WMO and the Ozone Issue, WMO No. 778, Geneva, Switzerland, 16 pp.